Heliyon 5 (2019) e01633

Contents lists available at ScienceDirect

Heliyon

journal homepage: www.heliyon.com

Heliyon

In vitro studies on gelatin/hydroxyapatite composite modified with osteoblast for bone bioengineering

Namrata Yadav, Pradeep Srivastava *

School of Biochemical Engineering, IIT (BHU), Varanasi, 221005, India

ARTICLE INFO

Keywords:
Bioengineering
Biotechnology

ABSTRACT

A promising route towards bone tissue engineering is made by the raw materials of the composite which mimics properties of the extracellular matrix components. Herein, the favourable human origin bone cells were seeded on the scaffold types to investigate the best co-culture system. The same has been achieved after the synthesis and characterization of gelatin/hydroxyapatite composites infused with chitosan for their calcium to phosphate (Ca/P) ratio by SEM-EDX. Also, *in vitro* biodegradation and bio-mineralization determined after immersing in lysozyme and SBF respectively. Uni-axial Compressive Strength (UCS), porosity, qualitative to quantitative phase development by XRD and FTIR were evaluated. The human bone cell-seeded composite was tested by flow cytometry, CLSM, SEM and DSC. This study statistically signified the human mesenchymal stem cell (hM) derived bone cell as potential raw material for minor to severe bone related tissue regenerative studies.

1. Introduction

As the world population ages, elderly patients face bone defect related morbidity and disability. This dramatically favour the need for regenerative bone development to improve overall health and so the quality of life. Today, common bone reconstruction practice incorporated for orthopaedic difficulties incur grafts [1]. As a conventional approach in the clinical setting with success rates touching ~90%, autografts suffer limited availability and donor implant site morbidity [2]. This has switched the focus to current alternative procedures available to reconstruct bone for trauma, tumor resection, and congenital skeletal diseases in addition to bone fracture. Bone tissue engineering revolutionizes the regeneration of bone to prominently improve the life of patients with severe bone defects [3]. In the regeneration of an injured organ, many tissue engineered biodegradable yet bio-mineralised biomaterial material based composites were proposed. During the past years, an extensively studied class of biomaterials has evolved in bone tissue engineering from both natural and synthetic in origin [2, 3], and when seeded with donor bone cell for use as bone graft stand a chance in successful bone repair. It is interesting to develop composite mimicking native extracellular matrix (ECM) because it is inspired by bone architecture [4]. Complex inorganic-organic composite structure defines bone ECM where non-stoichiometric inorganic hydroxyapatite crystals embed between collagen type I organic phase [5].

First, natural origin based biomaterials offer advantages of osteoconductivity, osteoinductivity, cytocompatibility and bioactivity in addition to native physiochemical properties, which bio-mimic the natural bone tissue [2]. These have been taken into account after human bone cell seeding onto the composites via Scanning Electron Microscopy (SEM), Fluorescence Activated Cell Sorter (FACS) and Confocal Laser Scanning Microscopy (CLSM). SEM was used to define the composite topography and cell attachment. Flow cytometry from FACS determines the potential proliferating population to be seeded in the scaffold and CLSM was done to evaluate composite biocompatibility all at different time points during the study.

Due to collagen by-products elicited immunogenic response, an alternate organic matrix component source was required as an option. Here, preferably gelatin was used as the organic component in composite preparation. Gelatin's role as matrix was studied upon its biodegradation when kept in lysozyme at physiological conditions. Gelatin is a linear, amorphous, hydrophilic and mouldable biomaterial in thermal solution directs DSC thermogram. It is biocompatible with relatively slower degradation rate with the by-products not being immunogenic at all [6, 7]. The property to support multiple interactions in the biological environment made it the favourite biomaterial among bone related methods [8, 9]. Hydroxyapatite with sufficiently good biocompatibility and fare mechanical property (UCS study) is reasonable to use as the structural framework component. It also promotes bioactivity supporting ECM to

* Corresponding author.
E-mail address: pksrivastava.bce@itbhu.ac.in (P. Srivastava).

https://doi.org/10.1016/j.heliyon.2019.e01633
Received 13 December 2018; Received in revised form 3 March 2019; Accepted 30 April 2019

grow *in vitro*, and when in Simulated Body Fluid (SBF) promote bio-mineralization.

With the combination of favourable properties, hydroxyapatite stood as the ideal inorganic component for the composite to be synthesised [10, 11, 12]. Chitosan, a semi-deacetylated chitin derivative is a non-toxic *in vivo* degradative by-products [13, 14]. It supports excellent bone cell adhesion to create microenvironment for ECM deposition [6] as evident from CLSM images [7, 8]. It holds promising biomaterial choice because of its low immunogenicity, biodegradability and biocompatibility [16].

The focus of this study is the comparison among human bone cell seeded-composites from the control group i.e. natural biomaterial based bone substitutes moulded from gelatin, hydroxylapatite and chitosan. These composites' preparation involves a freeze-dried slurry and lyophilisation method creating sites for bone cell differentiation and attachment. Bone cell from human origin were cultured on these composites *in vitro* to determine their applicability for bone tissue engineering [10]. Here, composites were expected to provide information for cell sustainability and hence ECM deposition to meet bone tissue engineering requirements.

2. Experimental

2.1. Materials

Gelatin, chitosan (degree of acetylation: 72.4%) and other solvents were purchased from Merck. For the *in vitro* studies, both hM (human bone marrow Mesenchymal Stem Cells/MSC differentiated bone cell) was purveyed by Institute of Medical Science, Banaras Hindu University (IMS, BHU), India.

The cells were cultured with low glucose-Dulbecco's modified Eagle's medium (DMEM) supplemented with 1% antibiotic-antimycotic solution (AAS), Non-Essential Amino-acid (NEA), osteogenic induction (high glucose DMEM, 10% FBS, 10nM dexamethasone (Dex), 10mM ß-glycerophosphate (ßGP), 1 μg/ml Bone Morphogenetic protein (BMP-2) and Ascorbic acid were supplied from Himedia (India)). Lysozyme, HCl, chloramines-T was purchased from Sigma.

2.2. Composite studies

Chitosan (C), gelatin(G) and hydroxyapatite(H) solution were prepared separately in acetic acid, distilled water at 40 °C and in Dimethyl Formamide to Trihydroxyfluoride (DMF:THF:1:5) respectively. This research study was performed for over a period of 28 culture days among four composite groups on the basis of raw material constituting part of the composite: CG (chitosan in gelatin matrix), GH (hydroxyapatite in gelatin matrix), CH (hydroxyapatite in chitosan) and CGH (chitosan and hydroxyapatite in gelatin matrix). Composition of the composites have been summarised in Table 1. Composite based composite slurry was prepared, then lyophilised at 40mm torr at -40 °C. The groups were studied *in vitro* for morphological, mechanical and physicochemical characterization. Equal weighting composites were UV-sterilised and seeded in-separate with hM under simulated physiological conditions (37 °C in High glucose DMEM at pH = 7.4) for *in vitro* studies.

Table 1
Composition of the biomaterials.

Raw material (Merck)	**Initial Concentration (%w/v)**		
Composite pH = 7.4	Chitosan/Chi in 2% acetic acid at RT 5% 'C'	Gelatine/Gel in DDW at 40 °C 10% 'G'	Hydroxylapatite/ Ha in DMF/THF (1:3) at RT, 13% 'H'
Sample	**Final concentration in the blend (%v/v)**		
CH #1 Control	35	-	40
CG #2	35	40	-
GH #3	-	40%	40%
CGH #4	35%	40%	20%

2.2.1. Morphology analysis

For SEM-EDX, harvested and seeded composite was mildly washed in PBS (pH 7.4), fixed overnight by 0.2M Sodium cacodylate in osteogenic media at 4 °C, later at room temperature dehydrated with graded increasing ethanol concentration (10%, 30%, 50%, 70% and 100%). Fixed in karnovsky fixative and air dried for 2h at room temperature before gold sputtering at 10mA for 5 min (Quarum Q150RES Penta FET Preunion) for SEM (ZEISS EVO/18 Research). SEM equipped EDX did spectrum analysis for calcium and phosphate.

Also, the collagen content was estimated by modified hydroxyproline assay based on hydrochloric acid from previous work [11].

2.2.1.1. In vitro degradation. The biodegradation of the lyophilised 2 × 1 cm CG, GH, CH and CGH composite based composites was studied by immersing them in lysozyme (10,000 U/mL) in DPBS (pH = 7.4) at 37 °C with 5% CO_2. After every 7 days, the composites were washed in MilliQ for removing the surface ions and lyophilised for SEM and TEM-SAED.

The average degradation rate of the composite was computed as follows:

$$\text{Degradation } \% = (W_i\text{-}W_d) / W_i \text{ X } 100 \text{ [12]}$$

Where, Wi is the initial dry weight before immersion and Wd is the sample dry weight measured after drying post-degradation. The degradation rate was noted as the mean ± SD (n = 5).

2.2.1.2. In vitro biomineralization. The biomineralization of 2 × 1 cm CG, GH, CH and CGH composite based composites was studied by immersing them in 1.5X SBF solution at 37 °C with 5% CO_2. The SBF solution was prepared as reported in previous work [9]. After every 7 days, composite samples were washed with 3X Milli Q for removing surface minerals., and later again lyophilised for SEM and TEM-SAED.

2.2.1.3. Porosity. The porosity of 2 × 1 cm CG, GH, CH and CGH composite based composites was studied by liquid displacement after immersing them in 5ml 99.9% ethanol for 7h in the graduated cylinder.

The composite porosity (ε) was measured as:

$$\varepsilon\ (\%) = (V_1 - V_3)/(V_2 - V_3) \text{ X } 100.$$

Where, V_1 is the initial ethanol volume, V_2 is the volume of ethanol soaked composite after 7h and V_3 is the residual ethanol volume after composite removal from the cylinder [13].

2.2.1.4. Uniaxial Compressive Strength (UCS) and thermal behaviour. The UCS of cylindrical composite (22mm diameter X 11mm length), were determined using TA5 cylinder (12.7mm Diameter and 35mm Length) by Texture analyser using Brookefield's CT3 10K, with a 9.81N load cell.

Differential Scanning Calorimetry (DSC) was done in Pyris 6 DSC's DSC 6000 to study the thermal behaviour of the biomaterialic composites after fixing the seeded scaffold with sodium cacodylate same as in SEM-EDX.

2.2.2. Chemical analysis

The crystal phase distribution in the lyophilised composite both with and without bone cell was determined from XRD (Rigaku D/Max-III X-RAY DIFFRACTOMETER with DIFFTECH software) using 0.717 nm Mo radiation generated at 40 kV and 30 mA. The sample was scanned at 2°/min from angular range 10°–60° in 2θ degrees. Composition dependent intermolecular interaction of the bone cell deposited and mineralized extracellular matrix (ECM) was studied by FTIR spectrophotometer (IRAffinity-1S SHIMADZU FTIR).

2.3. In vitro bone cell studies

2.3.1. Human bone cell seeding and culture on the composite

Isolated human MSC (Mesenchymal Stem Cell) were counted and cultured in the growth and differentiation medium respectively [14]. Cell were cultured in growth (low glucose DMEM supplemented with 1% AAS and NEA) and osteogenic induction (high glucose DMEM, 10% FBS, 10nM Dex, 10mM ßGP, 1 µg/ml BMP-2) medium at 5% CO_2 at 37 °C and water-saturated atmosphere [15].

Sterile equal weight composites (n = 5) were immersed and incubated in osteogenic induction media for 2 hours before seeding them in 24-well flat-bottom tissue-culture plates kept in humidified incubator at 37 °C, 5% CO_2. Later bone cell-seeded at composite were cultured and retrieved for *in vitro* studies.

2.3.2. In vitro bone cell attachment, proliferation and morphology

Hoechst 33258 labelled cells observed in Confocal Laser Scanning Microscopy (CLSM) in five regions at 63X. This defines cell morphology after seeding the composite via fluorescence indicating the loci of new bone deposition. From every experimental group (n = 5), washed intermittently in PBS (pH = 7.4) replacing DMEM and fixed by a droplet of 4% (v/v) formaldehyde, at 37 °C for 5 min. All sample sets were permeabilized with 500µl of 0.025% (v/v) Triton in PBS for 5 min. The 2 mL of 1% (v/v) FBS also in PBS used as the stopping solution for 20 min. For 5 min in the dark, 5 µL Hoechst 33258 in PBS at 1:100 ratio was added to each sample. Lastly, samples were dried after 3X PBS wash to view in CLSM [16].

FACS's flow cytometry quantifies the cellularity of the composite in the experimental groups [17]. In 1 µg/ml alexa flour 488, dye-positive living cells were evaluated for synchronous population to be studied on the composite by FACScan flow cytometer (BD™FACSCalibur) along with Cell Quest software.

2.4. Statistical Analysis

Statistical Analysis was performed using one-way ANOVA with a significance level of $p < 0.01$ in Graph pad prism version 5 software.

3. Results and discussion

3.1. Morphology analysis

Fig. 1 SEM-EDX compares the pore morphology and calcium to phosphate ratio in the raw materials used for preparing the biomaterials. To have biomaterial with higher porosity and balanced biodegradation to biomineralization, different permutations of raw material were studied. As it can be seen in Fig. 2, the cytochemical minerlization nodules were distinctly visible in human bone cell loaded on GH and CGH. Qualitatively SEM-EDX spectrum results indicated that bone cell preferentially adhered, spread and begin to proliferate into aggregates in all the experimental groups. After Day 21 of co-culture, when threshold cell concentration was achieved then cell spreading was evident in addition to Calcium-Phosphate based crystallization. As observed from SEM image (Fig. 2) elliptic aggregates are seen in CGH whereas circular in GH. SEM revealed dispersed cell attachment, proliferation, and mineralized layer deposition onto the composite [8]. These calcium and phosphate deposits contributed into increasing the crystallinity of bone cell seeded composite [18]. EDX spectrum from CGH displayed the Ca/P to be 1.67, closest to skeletal bone (Ca/P = 1.69) [19]. In the cell-seeded group, the prominent increase in Ca/P affected the morphology of the ECM coating as depicted in GH (Ca/P to 1.77) during this culture duration. The GH composite surface more prominently displayed hair-ball structures and was entirely covered by a dense collagen layer after Day 21 [20].

From the hydroxyproline assay, detectable presence of collagen was noted to be highest in hGH throught the culture duration. Findings from Figs. 1 and 2 are in accordance with EDX data indicating collagen deposition in parallel with rise in Ca/P in the scaffolds after cell seeding too.

Again, the EDX spectrum implied high calcium and phosphorous peak in the ECM mineral deposited on GH compared to CGH post-bone cell seeding (EDX spectrum from Fig. 4 and Table 2). Also from EDX, a recognizable decline in Ca/P (nearing Natural ideal bone Ca/P) accompanied with the rise of Ca and P % in the composite, supported strong Phosphate ion absorption. In the entire EDX spectrum, the occurrence of detectable carbon and oxygen peak emphasized by-product produced during ECM production. Based on relative %elemental comparison, the concentrations of carbon and oxygen are noted to be lower to that of Ca and P. The SEM micrographs showed that with chitosan loading, the surface roughness of the composites observed were likewise. The morphology change due to chitosan introduction and bone cell proliferation was evident in SEM Fig. 3. Plus, the EDX confirmed Ca/P nearing natural bone with a gain in culture days [21]. This result indicated that both GH and CGH composite might be suitable for bone tissue engineering.

3.1.1. In vitro degradation

The biodegradation of the composite was examined as one of the parameter affecting bone cell proliferation and expansion after cell seeding. Fig. 5 illustrates the effect of lysozyme in DPBS induced degradation on the biomaterials for a month when kept under

(a) G only

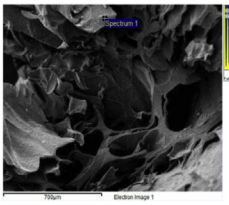

Element	Weight%	Atomic%
C K	43.88	54.32
O K	44.21	41.08
P K	1.67	0.80
Ca K	10.24	3.80
Totals	100.00	

(b) H only

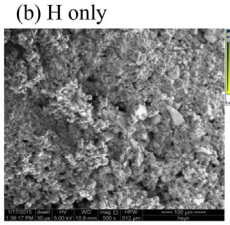

Element	Weight%	Atomic%
C K	72.30	75.96
O K	33.76	26.62
P K	1.24	0.39
Ca K	7.3	2.97
Totals	100.00	

(c) C ONLY

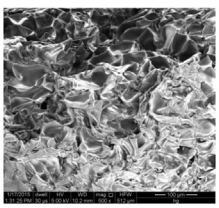

Element	Weight%	Atomic%
C K	67.22	73.20
O K	32.78	26.80
Totals	100.00	

(d) Calcium to phosphate ratio

Sr. No.	Sample	Ca/P
1.	Chitosan	-
2.	Gelatin	4.75
3.	Hydroxylapatite	5.88

Fig. 1. (a-c)SEM-EDX spectrum of individual raw material moulded composite (d) Comparative display of Ca/P from EDX spectrum.

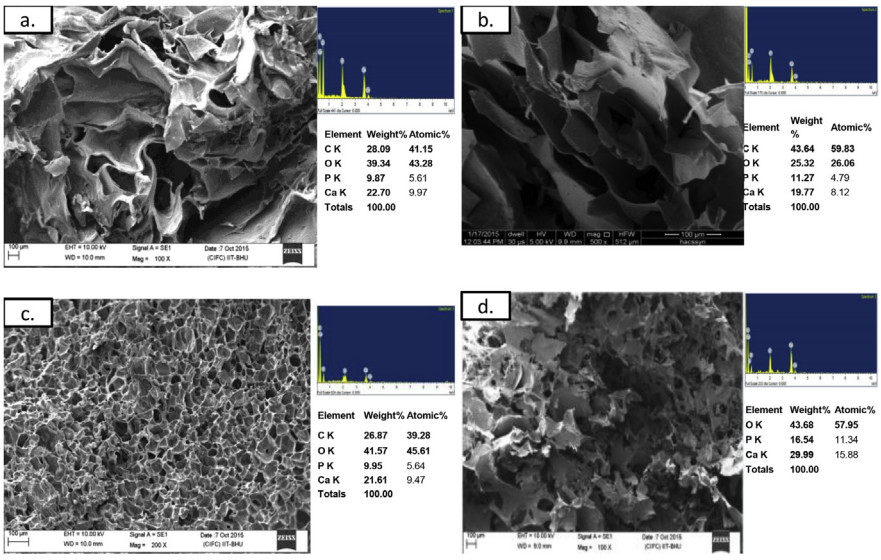

Fig. 2. SEM-EDX of the composites: (a) CG, (b) CGH, (c) CH and (d) GH.

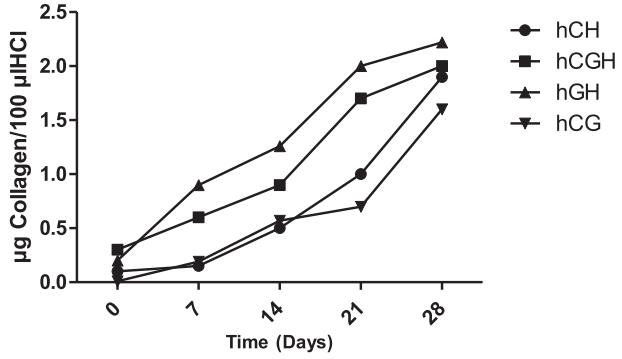

Fig. 3. The variation in collagen pattern after cell seeding in the scaffolds.

physiological conditions. All the composite composites degraded linearly during this degradation period. The degradation percentage was nearly 10–15% every week. The weight loss percentage of CG was nearing complete degradation unlike others where CGH displays step-well degradation upto 80% till day 30 upon hydroxyapatite introduction into the composite. Probably in the presence of lysozyme, the composite macromolecules preferentially degraded into smaller molecules soluble in DPBS. The CH composite with gelatin degraded more than the ones without gelatin. This observation pointed out the effect of varying the gelatin concentration would modify the degradation percentage.

Table 2
Comparative display of EDX based elemental analysis via Ca to P ratio.

Sr.no.	Sample Name	Ca/P in terms of Atomic wgt (%)
1.	GH	1.77
2.	CGH	1.67
3.	CH	1.692
4.	CG	1.400
5.	C	Absent
6.	G	4.75
7.	H	5.88

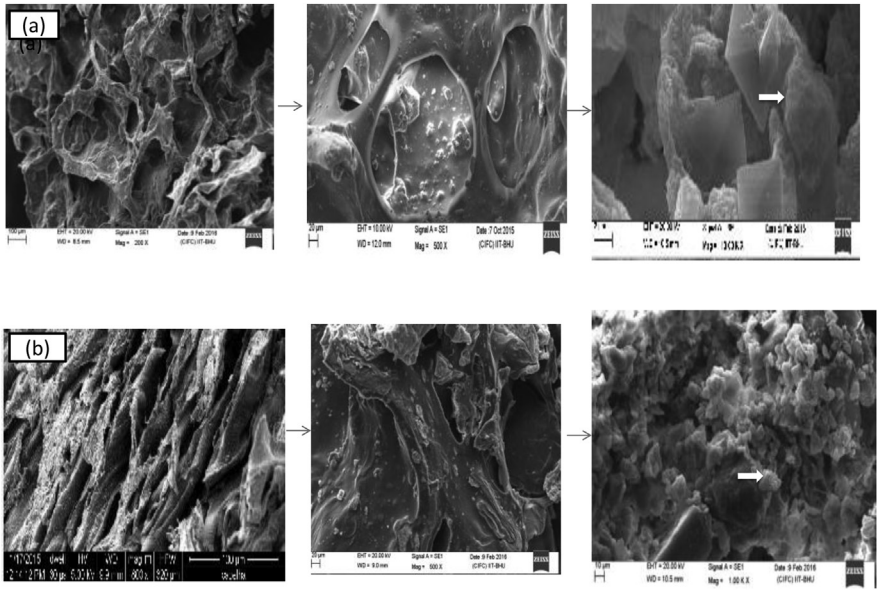

Fig. 4. SEM of cell seeded composite showing cytochemical mineralized nodules visible as Ca & P deposits (a) hGH and (b) hCGH.

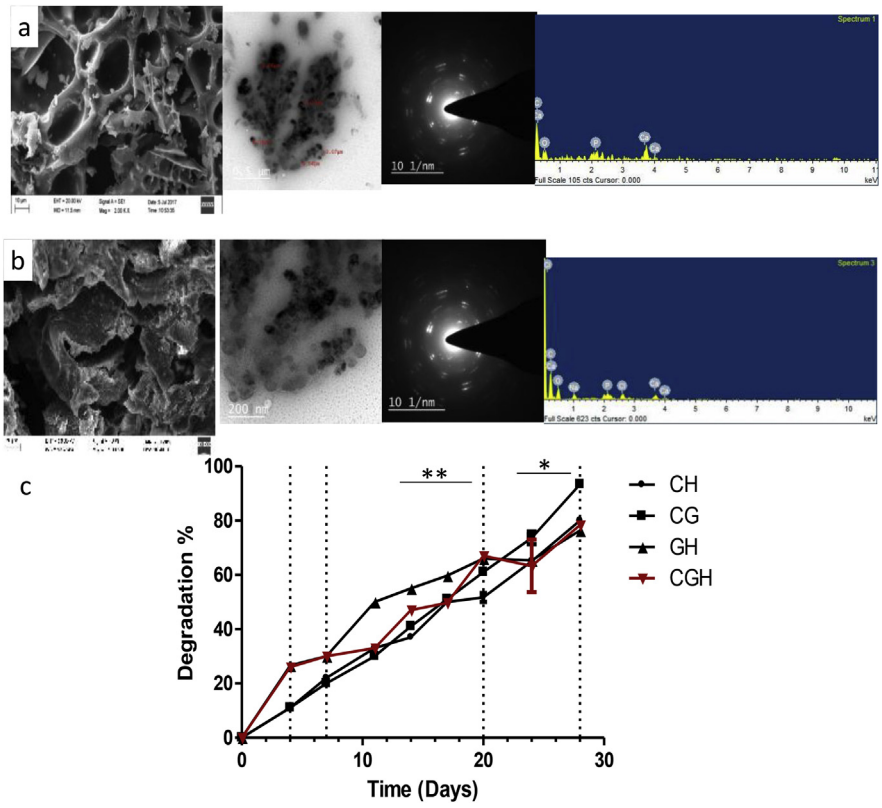

Fig. 5. SEM, TEM-SAED images of composites (a) GH and (b) CGH showing (c) Biodegradation as a function of time after immersed in lysozyme. **P < 0.01, *P < 0.0001.

3.1.2. *In vitro biomineralization*

These composites hold great potential in promoting biomineralization under physiological conditions in SBF solution. In 1.5X SBF, mineral deposition was observed after 7 days among all the composites from SEM and TEM-SAED in Fig. 6. The displayed apatite layers showed prominent crystalline behaviour specifically in CGH after day 14 in SBF. EDX spectrum displayed higher Ca/P ratio favouring mineral deposition in the pores also after day 14 in SBF. The mass

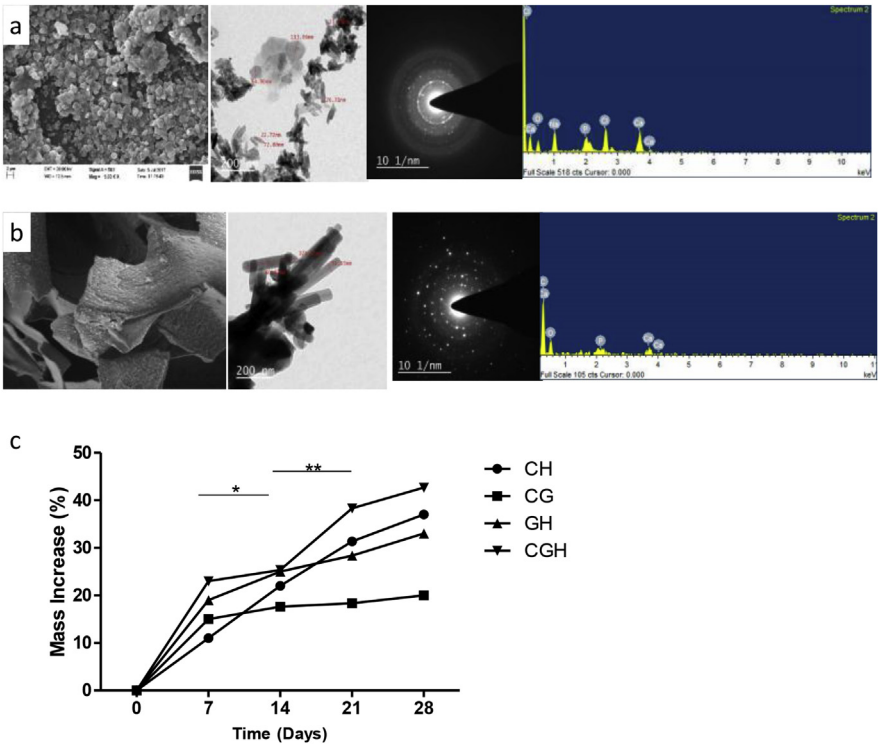

Fig. 6. SEM, TEM-SAED images of composites (a) GH and (b) CGH showing (c) Biomineralization as a function of time after immersed in SBF. **P < 0.01, *P < 0.0001.

increase was nearing 50% after about 4 weeks in SBF. This was attributed mainly to creation of mineral nucleation site from the hydroxyapatite particles in the composite. Due to the same, least deposition was observed in CG among the composite composites. This also supports hydroxyapatite presence contributed to composite bioactivity [5].

3.1.3. Uniaxial Compressive Strength (UCS) and porosity

Here, UCS was calculated to determine the mechanical strength of the composite studied. From Fig. 7A, the UCS was calculated for the composite and showed that the average of the result improved with chitosan introduction in GH. Hence, mechanical property decreased with increasing pore size for these composites. The supporting framework of the composite composite must have enough porosity supporting ECM deposition.

The porosity of all the composites was nearly 80%, less than theoretical value noted for the solid content (~95%). This slight change in the average porosity could be due of rearrangement in macromolecules during composite slurry preparation. From Fig. 7B the calculated porosity of the composite being ≤80% suggested ambient place supporting bone cell anchorage, attachment and proliferation. The porosity percentage was observed to be highest in CGH than the others. GH was found to be of suitable average porosity favouring cell ECM deposition. The interconnected porous structure enhanced mass transfer favouring cell communication and hence proliferation.

Also balanced porosity to mechanical strength favours selection of optimal composite based composite biomaterial for bone tissue engineering [22].

3.1.4. Thermal behaviour

DSC was done to evaluate the thermal behavior of human bone cell seeded-composite. The fraction of hydroxyapatite determined the degree of crystalline behaviour in the composites [23]. From DSC thermograms shown in Fig. 8, the intensity of the exothermic peak increased with hydroxyapatite inclusion as the composite component. Also, the recrystallization phenomenon was distinctly visible in CGH but become negligible in the other composites. Fig. 8 show that the endothermic effect among the composites after 200 °C was associated with the melting temperature of gelatin. In addition, along the same curve, characteristic peak of hydroxyapatite were observed. The cold crystallization temperature (Tcc) of CG biomaterial composite increased initially with the increase in gelatin content. Hydroxyapatite inclusion promoted drop in Tcc with increase in its concentration in the composite due to decrease in contact within the gelatin based matrix. Also, multiple melt peaks were observed in CGH-DSC decreased to distinct two peaks after bone cell seeding. The glass transition temperature (Tg) in CGH being the lowest, likely because of the size, hydroxyapatite crystal phase was consistently reduced but later strengthened because of the cell-matrix interactions after cell seeding. This indicates that hydroxyapatite could act as the nucleation site for crystallization in the composite, whereas in GH with no chitosan resulted in slower decomposition with the pattern being distinct than the other composites in the study group. The endothermic peak observed only in CG was associated with melting temperature of chitosan. The same being absent in GH but negligibly present in CH and CGH.

3.2. Chemical analysis

3.2.1. XRD

SEM and XRD investigated bone cell deposited Extracellular matrix calcium-phosphate (Ca-P) crystals at the micro and macroscopic level respectively. In accordance, XRD plotted in Fig. 9A shows that the primary phase was hydroxyapatite based. These results confirmed that the GH and CGH had bioactivity and might be positive in replacing natural human bone. The XRD results of the bone cell loaded composite in Fig. 9B displayed peaks none observed before bone cell seeding. Peaks associated with the crystalline inorganic hydroxyapatite were prominently detected. Their relative intensity rose enormously in CGH in comparison to GH in synchronisation with EDX Ca/P ratio (Table 2). From Fig. 9A, CH has inherited maximum crystalline behavior among all the composites followed by CGH. CH exceeded in being brittle with increase in crystallinity exceeding the threshold value for natural human bone. After composite fabrication in GH, the crystallite inorganic hydroxyapatite role decreased

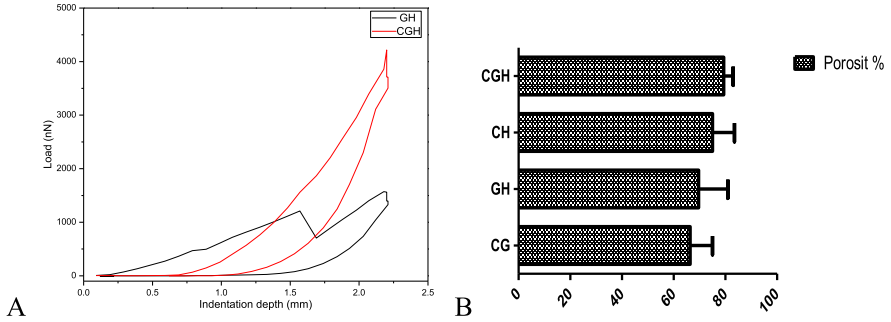

Fig. 7. A. Uniaxial Compressive Strength of GH and CGH and B. Comparative analysis of composite porosity.

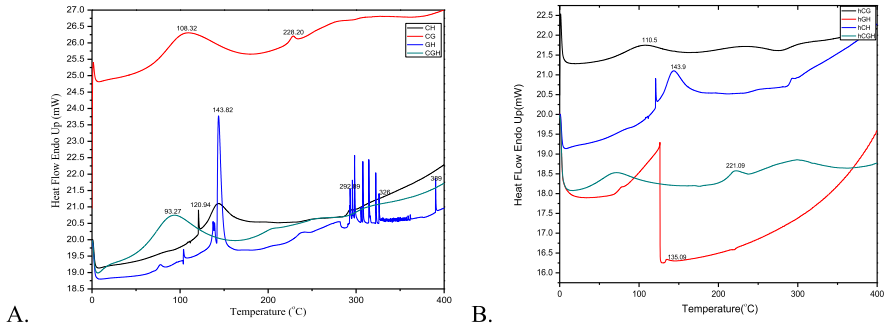

Fig. 8. DSC curves of scaffold A. Before and B. After cell seeding.

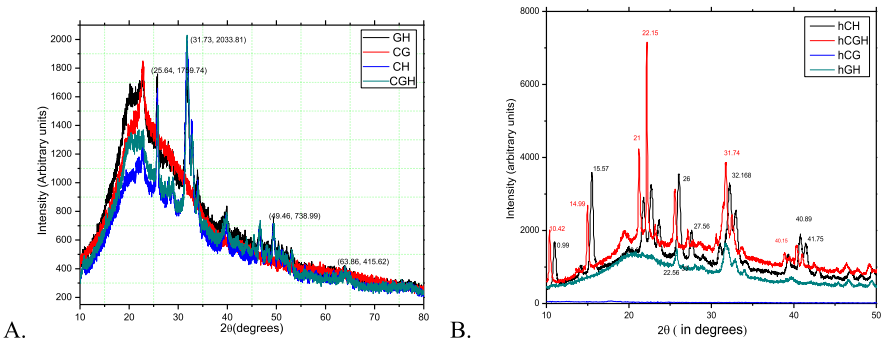

Fig. 9. XRD demonstrating quantitative phase development on the composite A. Composite without osteoblast and B. Osteoblast seeded composite.

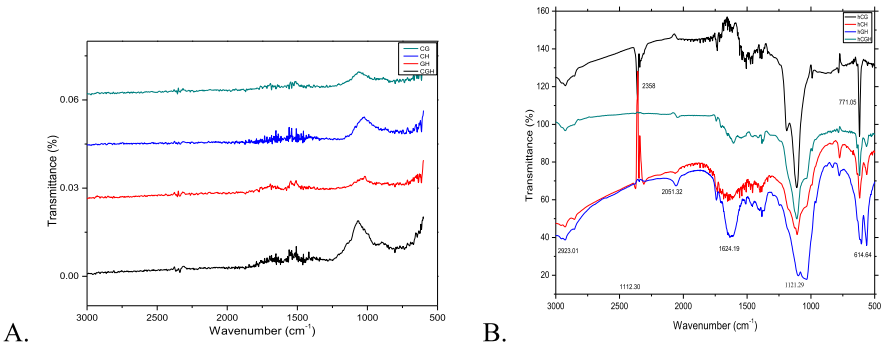

Fig. 10. Quanititative FTIR spectra of composite A. Composite without osteoblast and B. Osteoblast seeded composite.

in the composite, meanwhile increased post-seeding as shown in Fig. 9B. The characteristic Ha peaks were present but not altered significantly among groups studied, result from inorganic phase development around gelatin matrix. The arbitrary units (a.u.) in bone cell seeded CH and CGH became sharper and stronger in intensity in comparison to CG and GH. The shift, decrease in intensity, and missing intensities (e.g., $2\theta = 40^{\circ}$ in CH peaks were narrower and prominent than in CGH) of the consecutive peak of the composite and hinted towards bonding between gelatin matrix, Ha, and chitosan. It showed chitosan's role in increasing bonding peak intensities nearly by five times, by bonding with Ha in Gel matrix.

3.2.2. FTIR

FTIR interpretation confirmed the crystalline percentage and physicochemical properties which enable peak shifting indicating molecular interaction. FTIR of cells was done to know the mineral phase constitution deposited by cells upon co-culture. As the functionally active group engaged in bond formation, for the cell-seeded composite an the increase in peak intensities was observed unlike primarily decrease transmittance in the composite without cells Fig. 10. FTIR data revealed the critical information about interactions between the Ha-based dispersed inorganic phase and the Gelatin-based matrix both with and without bone cell seeding. These composite demonstrated overlapping FTIR characteristic peaks but with peak shift and the difference in peak intensity, presented in Fig. 10A.

Distinct bands were observed for the cell-seeded composites. The sharp peak at 614 corresponded to phosphate group stretch vibration after ECM coating. The strong peak at 771 was related to Amide IV mainly 0 = C-N deformation. The sharp peak at 1112 was related to ester C-O asymmetric stretch. Meanwhile, hCH showed the only prominent peak at 1624 (variable intensity C=C stretch, Amide I, II, III) unlike the other 3 in the cell-seeded group. Crystalline hydroxyapatiite contained carbonate ions at $1624cm^{-1}$. The peak at 2051 corresponds to C=O stretch, The peak at 2358 was also reported in high-temperature extracted gelatin which displayed distinct amide III peaks like bone gelatin [24]. The medium peak at 2923 is for C-H stretch.

However, there was a significant difference between the spectra: the characteristic peak of carbonate group at 771 cm^{-1} nearly disappeared in the hCGH (Fig. 10B). In contrast, the CG based matrix showed higher intensity w.r.t. the rest of the composites at 1121.29 which indicated a strong vibration due to C-O and C-N stretch. This bond may be indicative of active bonding between calcium ions and carbonyl (C-O) bonds.

Peak shift observed from 1930-2070 corresponds to C=N stretching vibration from the formation of water-nitrile complexes. This exciting phenomenon strongly favoured the configuration of GH and CGH. In the absence of hydrophilic chitosan, the fingerprint region showed shallow peaks. More groups in the Gelatin-based matrix begin to assemble with chitosan addition [25].

3.3. Bone cell studies

3.3.1. In vitro bone cell attachment, proliferation and morphology

From the cell cycle analyzed, the percentage of cells in the G0/G1, S and G2/M phase determined by alexa flour 488-FACS on bone cell groups as shown in Fig. 11a. hM showed the higher proliferative population in S phase compared to hT when the unstained population was used as a control. Hoechst33258-nuclear staining of live cells and alexa flour 488-cytoskeleton staining was done after day 14 in culture to determine cell attachment. The cell proliferation was observed in the cell-seeded composite by CLSM (Fig. 11c–g). Bone cell seeded on GH and CGH showed well-spread morphology unlike on CH and CG. The CLSM results showed that in bone cell were partly-attached to the composites and have round shape in hCG and hCH Fig. 11d–e. In GH and CGH, the cells were attached completely, displaying branched morphology and hence nontoxicity of composite. From the FACS and CLSM data, GH and CGH were selected for cell seeding.

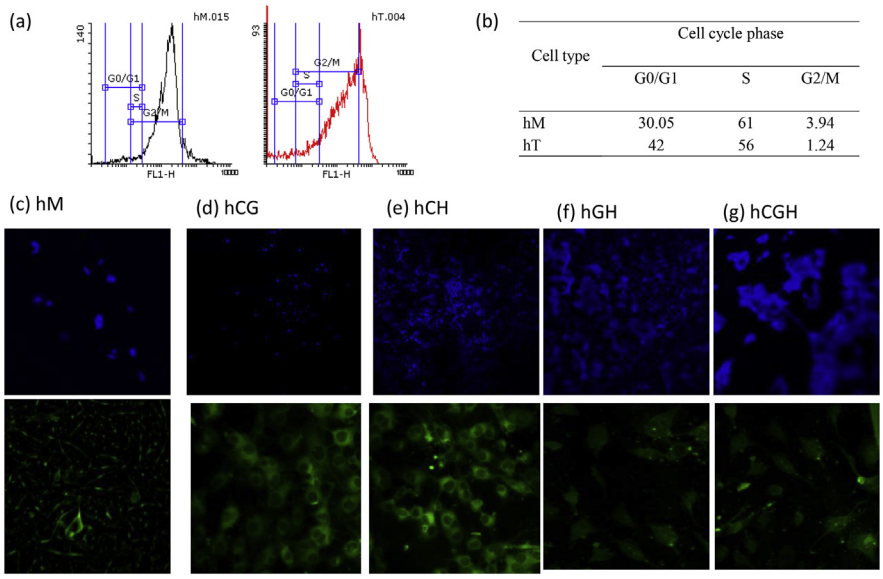

Cell type	Cell cycle phase		
	G0/G1	S	G2/M
hM	30.05	61	3.94
hT	42	56	1.24

Fig. 11. FACS analysis of (a–b) Human osteoblast cell cycle analysis and CLSM Hoechst 33258 labelled nuclei and alexa flour 488 labelled ECM in the osteoblast seeded composites (c) hM, (d)hCG, (e) hCH, (f) hGH and (g) hCGH.

4. Conclusion

Natural process of biomineralization with the freeze-dried chitosan infused gelatin-hydroxyapatite biomaterial was studied in the assessment of its biocompatibility and bioactivity using human-origin based bone cell obtained from differentiated bone marrow MSC (hM). The synthesised novel biocomposite mimics the extracellular matrix of the bone, hence, the morphological and mechanical properties of the biocomposite directly influences the healing step employing bone tissue engineering. From the EDX spectrum, Ca/P ratio observed to be closer to that of natural bone in 'CGH' composite. Porosity to UCS, mineralization and degradation properties also improved with all the three raw materials present. Additionally crystalline behaviour proved to be more prominent in CGH as observed in XRD. The chitosan infused showed quite better biomineral activity when seeded with hM. The incorporation of chitosan into GH based composite increased the hM viability and activity over GH with hT. Ca-P deposition with the increase in culture duration was reflective of the stimulated differentiation ability of hM. In future, the *in vivo* cell studies over time would reflect the properties of the substrate suitable for bone tissue engineering involving hM.

Declarations

Author contribution statement

Namrata Yadav: Conceived and designed the experiments; Performed the experiments; Analyzed and interpreted the data; Wrote the paper.

Pradeep Srivastava: Conceived and designed the experiments; Analyzed and interpreted the data; Contributed reagents, materials, analysis tools or data.

Funding statement

This research did not receive any specific grant from funding agencies in the public, commercial, or not-for-profit sectors.

Competing interest statement

The authors declare no conflict of interest.

Additional information

No additional information is available for this paper.

Acknowledgements

The original field work was supported by IIT BHU, Varanasi. The authors gratefully acknowledge support from IMS, BHU, Varanasi for this study in terms of human cell source availability. The authors also thank Dr. Geeta Rai, Centre of Human and Genetic Resources BHU, Varanasi for the technical support. The authors thank Department of Metallurgy, IIT BHU, NIT Trichy, India and BHU for chemical analysis, DSC and FACS-CLSM facility respectively. Authors thank Ms. Reena Vishvakarma, School of Biochemical Engineering, IIT BHU for proof reading the manuscript.

References

[1] B. Noorani, F. Yazdian, A. Khoshraftar, R. Vaez Ghaemi, Z. Alihemmati, H. Rashedi, S. Shahmoradi, Fabrication and evaluation of nanofibrous polyhydroxybutyrate valerate scaffolds containing hydroxyapatite particles for bone tissue engineering, Int. J. Polym. Mater. Polym. Biomater. 0 (2018) 1–9.

[2] N. Shadjou, M. Hasanzadeh, B. Khalilzadeh, Graphene based scaffolds on bone tissue engineering, Bioengineered 5979 (2017), 00–00.

[3] Z. Chen, Y. Song, J. Zhang, W. Liu, J. Cui, H. Li, F. Chen, Laminated electrospun nHA/PHB-composite scaffolds mimicking bone extracellular matrix for bone tissue engineering, Mater. Sci. Eng. C 72 (2017) 341–351.

[4] D. Mishra, B. Bhunia, I. Banerjee, P. Datta, S. Dhara, T.K. Maiti, Enzymatically crosslinked carboxymethyl – chitosan/gelatin/nano-hydroxyapatite injectable gels for in situ bone tissue engineering application, Mater. Sci. Eng. C 31 (2011) 1295–1304.

[5] M. Shakir, R. Jolly, M.S. Khan, A. Rauf, S. Kazmi, Nano-hydroxyapatite/β-CD/chitosan nanocomposite for potential applications in bone tissue engineering, Int. J. Biol. Macromol. 93 (2016) 276–289.

[6] L. Pighinelli, M. Kucharska, Chitosan – hydroxyapatite composites, Carbohydr. Polym. 93 (2013) 256–262.

[7] B. Hakan, B. Buyuk, M. Huysal, S. Isik, M. Senel, W. Metzger, G. Cetin, Preparation and characterization of amine functional nano-hydroxyapatite/chitosan bionanocomposite for bone tissue engineering applications, Carbohydr. Polym. 164 (2017) 200–213.

[8] A. Teimouri, M. Azadi, Preparation and characterization of novel chitosan/nanodiopside/nanohydroxyapatite composite scaffolds for tissue engineering applications, Int. J. Polym. Mater. Polym. Biomater. 65 (2016) 917–927.

[9] M.R. Nikpour, S.M. Rabiee, M. Jahanshahi, Composites : Part B Synthesis and characterization of hydroxyapatite/chitosan nanocomposite materials for medical engineering applications, Compos. Part B. 43 (2012) 1881–1886.

[10] J. Salgado, O.P. Coutinho, R.L. Reis, Bone Tissue Engineering : State of the Art and Future Trends, 2004, pp. 743–765.
[11] C. Content, K.A. Athanasiou, J.M. Link, J.C. Hu, A modified hydroxyproline assay based on hydrochloric acid in Ehrlich's solution, Accurately Meas. Tissue 23 (2017) 243–250.
[12] M. Swetha, K. Sahithi, A. Moorthi, N. Srinivasan, International Journal of Biological Macromolecules Biocomposites containing natural polymers and hydroxyapatite for bone tissue engineering, Int. J. Biol. Macromol. 47 (2010) 1–4.
[13] N. Johari, H.R. Madaah Hosseini, A. Samadikuchaksaraei, Novel fluoridated silk fibroin/TiO2nanocomposite scaffolds for bone tissue engineering, Mater. Sci. Eng. C 82 (2018) 265–276.
[14] N. Ye, S. Suttapreyasri, S. Kamolmatyakul, ScienceDirect Comparative study of different centrifugation protocols for a density gradient separation media in isolation of osteoprogenitors from bone marrow aspirate, JOBCR 4 (2014) 160–168.
[15] A. Us, A. Ab, Method and Means for Culturing Osteoblastic Cells, 2016, pp. 1–9.
[16] D. Jing, M. Zhai, S. Tong, F. Xu, J. Cai, G. Shen, Y. Wu, X. Li, K. Xie, J. Liu, Q. Xu, E. Luo, Pulsed electromagnetic fields promote osteogenesis and osseointegration of porous titanium implants in bone defect repair through a Wnt/β-catenin signaling-associated mechanism, Sci. Rep. 6 (2016) 1–13.
[17] S. Post, B.M. Abdallah, J.F. Bentzon, M. Kassem, Demonstration of the presence of independent pre-osteoblastic and pre-adipocytic cell populations in bone marrow-derived mesenchymal stem cells, Bone 43 (2008) 32–39.
[18] C. Vaquette, S. Ivanovski, S.M. Hamlet, D.W. Hutmacher, Biomaterials Effect of culture conditions and calcium phosphate coating on ectopic bone formation, Biomaterials 34 (2013) 5538–5551.
[19] P. Wang, L. Zhao, J. Liu, M.D. Weir, X. Zhou, H.H.K. Xu, Bone Tissue Engineering via Nanostructured Calcium Phosphate Biomaterials and Stem Cells, 2014.
[20] M. Haeri, M. Haeri, ImageJ Plugin for analysis of porous scaffolds used in tissue engineering, J. Open Res. Softw. 3 (2015) 2–5.
[21] M. Nouri-felekori, A.S. Mesgar, Z. Mohammadi, Development of composite scaffolds in the system of gelatin À calcium phosphate whiskers/fi brous spherulites for bone tissue engineering, Ceram. Int. 41 (2015) 6013–6019.
[22] C. Gandhimathi, J.R. Venugopal, A.Y. Tham, S. Ramakrishna, S.D. Kumar, Biomimetic hybrid nanofibrous substrates for mesenchymal stem cells differentiation into osteogenic cells, Mater. Sci. Eng. C 49 (2015) 776–785.
[23] S. Eftekhari, I. El, Z. Shaghayegh, G. Turcotte, H. Bougherara, Fabrication and characterization of novel biomimetic PLLA/cellulose/hydroxyapatite nanocomposite for bone repair applications, Mater. Sci. Eng. C 39 (2014) 120–125.
[24] P. Garidel, H. Schott, Fourier-Transform midinfrared spectroscopy for analysis and screening of liquid protein formulations Part 2: details analysis and applications, Bioprocess Int. 1 (2006) 48–55.
[25] J.H. Muyonga, Fourier transform infrared (FTIR) spectroscopic study of acid soluble collagen and gelatin from skins and bones of young and adult Nile perch (Lates niloticus), Food Chem. 86 (2004) 325–332.